Diagn Interv Radiol 2025; DOI: 10.4274/dir.2025.253324

ABDOMINAL IMAGING

ORIGINAL ARTICLE

Multiparametric magnetic resonance imaging, diffusion-weighted magnetic resonance imaging, and magnetic resonance elastography: differentiating benign and malignant liver lesions

Avaz Jabiyev
Muşturay Karçaaltıncaba
Ali Devrim Karaosmanoğlu
Deniz Akata
Mustafa Nasuh Özmen
İlkay Sedakat İdilman

Hacettepe University Faculty of Medicine, Department of Radiology, Ankara, Türkiye

PURPOSE

This study investigates the accuracy of multiparametric magnetic resonance imaging (mpMRI), diffusion-weighted imaging (DWI), and magnetic resonance elastography (MRE) in differentiating benign and malignant liver lesions.

METHODS

This retrospective study included patients with focal liver lesions who underwent MRI and MRE between 2018 and 2022. Based on histopathologic analyses or follow-up imaging findings, 70 solid liver lesions were retrospectively evaluated as benign (n = 20) or malignant (n = 50).

RESULTS

There was no statistically significant difference between the benign and malignant liver lesions in pre-contrast T1 relaxation times ($P > 0.05$). Malignant liver lesions had a significantly lower T2 value, contrast-enhancement ratio (CER), T1 relaxation time reduction (T1D), T1D percentage [T1D (%)], and apparent diffusion coefficient (ADC), along with a significantly higher stiffness value ($P < 0.05$). In receiver operating characteristic analysis, the following cut-off values were determined for differentiating malignant from benign lesions: a CER of 1.99 [area under the curve (AUC): 0.828, sensitivity 78.6%, specificity 73.2%], a T1D of 749.5 ms (AUC: 0.817, sensitivity 71.4%, specificity 78%), a T1D (%) reduction of 49.71% (AUC: 0.831, sensitivity 78.6%, specificity 73.2%), a T2 relaxation time of 74 ms (AUC: 0.705, sensitivity 65%, specificity 76.6%), an ADC of 1.275×10^{-3} mm^2/s (AUC: 0.861, sensitivity 89.5%, specificity 81.2%), and a stiffness of 3.77 kPa (AUC: 0.848, sensitivity 85%, specificity 75%).

CONCLUSION

Combined mpMRI, DWI, and MRE provide high diagnostic accuracy, with ADC and MRE offering superior performance in differentiating malignant from benign liver lesions.

CLINICAL SIGNIFICANCE

This article highlights the accuracy of mpMRI, MRE, and DWI in distinguishing between malignant and benign liver lesions. These findings support the integration of mpMRI, DWI, and MRE into clinical practice for non-invasive liver lesion characterization.

KEYWORDS

Multiparametric magnetic resonance imaging, liver, diffusion-weighted imaging, magnetic resonance elastography, focal lesion

Corresponding author: İlkay Sedakat İdilman

E-mail: isidilman@hacettepe.edu.tr

Received 16 March 2025; revision requested 10 April 2025; accepted 28 April 2025.

Epub: 03.06.2025

Publication date: 02.03.2026

DOI: 10.4274/dir.2025.253324

You may cite this article as: Jabiyev A, Karçaaltıncaba A, Karaosmanoğlu AD, Akata D, Özmen MN, İdilman İS. Multiparametric magnetic resonance imaging, diffusion-weighted magnetic resonance imaging, and magnetic resonance elastography: differentiating benign and malignant liver lesions. *Diagn Interv Radiol*. 2026;32(2):133-138.

The detection of focal liver lesions (FLLs) is one of the most commonly encountered findings in abdominal imaging in clinical practice. Although the majority of liver lesions in non-cirrhotic livers are benign, an FLL can sometimes represent the first indication of metastatic liver disease from an unknown primary malignancy. Since management strategies differ substantially based on the lesion's nature, it is crucial to differentiate malignant lesions from benign ones. Although specific imaging characteristics are associated with typical benign and malignant FLLs, atypical findings may complicate diagnoses and cause unnecessary anxiety for both patients and physicians.

Magnetic resonance imaging (MRI) is recognized as the most accurate radiological method for characterizing liver lesions.[1] MRI examinations routinely incorporate diffusion-weighted imaging (DWI) along with conventional sequences, using gadolinium-based extracellular or hepatospecific contrast agents in post-contrast multiphase studies to evaluate FLLs. Although hepatospecific contrast agents share properties with extracellular agents in dynamic imaging, the additional diagnostic information obtained during the hepatospecific phase enhances the differential diagnosis of liver lesions and improves the detection of small FLLs.[2] The combination of apparent diffusion coefficient (ADC) values, which decrease in malignancy, further improves the accuracy of MRI in characterizing FLLs.[3] Emerging MRI techniques in liver imaging, such as multiparametric MRI (mpMRI)–including T1, T2, and T2* mapping–and magnetic resonance elastography (MRE), have proven effective in imaging diffuse liver diseases.[4-6] However, the literature includes limited studies evaluating the characteristics of MRE and mpMRI and their roles in differentiating FLLs.[7-9] In this retrospective study, we aimed to demonstrate the mpMRI, MRE, and DWI characteristics of FLLs and evaluate the role of these quantitative measures in their characterization.

Main points

- Emerging magnetic resonance imaging techniques can effectively aid in distinguishing between malignant and benign liver lesions.
- Malignant liver lesions exhibit significantly lower T2, contrast-enhancement ratio, T1 relaxation time reduction (T1D), T1D percentage, and apparent diffusion coefficient (ADC) values while showing notably higher stiffness values.
- ADC values and lesion stiffness demonstrate slightly better performance in differentiating malignant from benign liver lesions.

Methods

This retrospective study received approval from the Hacettepe University Ethics Committee on July 26, 2022 (GO 22/380). A total of 50 patients with 70 lesions who underwent liver MRI, MRE, and mpMRI between January 1, 2018, and February 21, 2022, were included. Indications for MRI included suspicion of an FLL on ultrasound or computed tomography, follow-up imaging for chronic liver disease, and preoperative or follow-up imaging in patients with primary tumors outside the liver. Patients under 18 years of age; those who had undergone chemoembolization, radioembolization, or radiofrequency ablation; and those with lesions smaller than 1 cm (to avoid partial volume artifacts) were excluded from the study (Figure 1).

Magnetic resonance imaging examinations

All MRI examinations were performed on a 1.5-T system (Magnetom Aera, Siemens Healthcare, Erlangen, Germany). A 30-channel phased-array body coil was used, and patients were scanned in the supine position. All patients underwent MRI after a fasting period of 4–6 hours. A 3-plane localization gradient echo sequence was performed at the beginning of the examination. The standard liver MRI protocol included in-phase and out-of-phase sequences, coronal T2 HASTE, axial fat-suppressed T2, DWI, axial 3D dynamic T1, and axial and coronal hepatobiliary phase images obtained at the 20th minute after administration of Gd-EOB-DTPA (Primovist; Bayer-Schering Pharma AG, Berlin, Germany).

DWI and ADC mapping were performed at b-values of 50, 400, and 800 s/mm^2. The sequence parameters were as follows: a repetition time (TR) of 6200 ms, an echo time (TE) of 54 ms, a flip angle of 60°, a field of view (FOV) of 380 × 300 mm^2, a slice thickness of 8 mm, a matrix size of 192 × 144, a number of excitations (NEX) of 3, and a total acquisition time of 3 minutes.

Furthermore, T1 mapping was conducted using a B1 inhomogeneity-corrected method with variable flip angles. The sequence parameters were as follows: a TR of 4.4 ms, a TE of 2.1 ms, flip angles of 3° and 15°, a matrix size of 256 × 156, a FOV of 380 × 300 mm, a slice thickness of 4 mm, and an acquisition time of 1.5 minutes. For T2 mapping, various TEs were used with an SSFP-based true fast imaging with steady precession sequence and an exponential signal decay model. The parameters were as follows: a TR of 166 ms; TEs of 0, 25, and 55 ms; a flip angle of 70°; an FOV of 420 × 260 mm; a slice thickness of 10 mm; a matrix size of 192 × 192; a NEX of 1; and an acquisition time of 1.2 minutes. In addition, T2* mapping, used to evaluate hepatic iron load, was performed with the following parameters: a TR of 200 ms; TEs of 0.93, 2.1, 3.35, 4, 4.56, 5.77, 6.98, 8.19, 9.4, 10.61, 11.82, 13.03, and 14.24 ms; a flip angle of 20°; a slice thickness of 10 mm; an FOV of 400 × 300 mm; and a matrix size of 160 × 85.

MRE was performed using an active driver that generated mechanical waves at 60 Hz and a modified 2D gradient-recalled echo

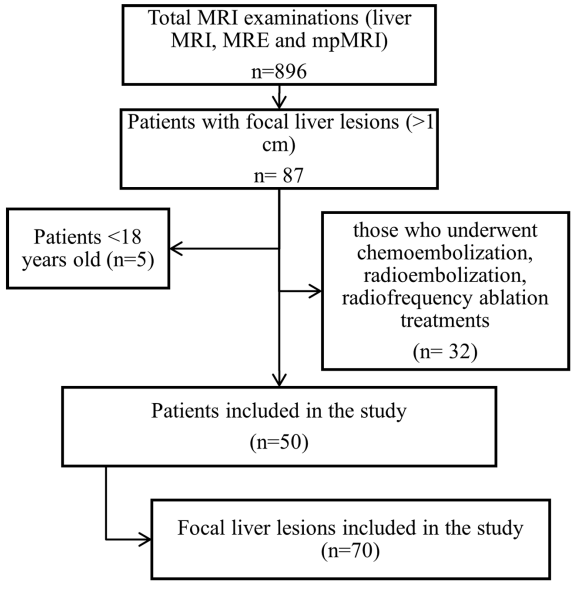

Figure 1. Study flowchart. MRI, magnetic resonance imaging; MRE, magnetic resonance elastography; mpMRI, multiparametric magnetic resonance imaging.

sequence. The sequence parameters were as follows: a TR of 50 ms, a TE of 21 ms, a flip angle of 25°, a bandwidth of 31.25 kHz, a matrix size of 256 × 128, and an acquisition time of 2.5 minutes. Depending on liver size, four slices, each 10-mm thick, were obtained from the largest portion of the liver during a breath-hold. All MRI, mpMRI, MRE, and DWI sequences were performed during the same imaging session.

Imaging analysis

All data were transferred to a workstation (Syngo.via Siemens, Erlangen, Germany) for analysis. The MR images were reviewed by one radiologist (A.J., with 5 years of experience) under the supervision of a senior radiologist with 16 years of experience (I.S.I.). Lesion measurements were performed using a free-hand region of interest (ROI) that included a sufficiently large portion of the lesion while maintaining a thin margin outside the lesion's periphery to avoid partial volume artifacts. Free-hand ROIs were also drawn on the magnitude images to include FLLs and were copied onto the stiffness map, which provided liver stiffness values in kPa.

The average T1 relaxation time values before and after contrast–pre-contrast (pre-T1 value) and at 20 minutes post-contrast on hepatobiliary phase images (post-T1 value)–were used to calculate the contrast-enhancement ratio (CER), as previously described by Yoshimura et al.[10] Additionally, the decrease in T1 relaxation time [T1 relaxation time reduction (T1D)] and the percentage reduction in T1 relaxation time [T1D (%)] were calculated from these measurements, as outlined by Peng et al.[11] Subsequently, ADC values were calculated for the lesions using diffusion-weighted images. This measurement was performed using an ROI that included a sufficiently large portion of the lesion while preserving a thin margin outside the lesion's periphery on the ADC mapping images, in consensus with two experienced readers (A.J. and İ.S.İ.).

Statistical analysis

Statistical analysis was performed using SPSS version 23.0 (IBM Inc., Armonk, NY, USA) and Microsoft Excel (Microsoft Corporation, 2018). Categorical variables were summarized as counts and percentages, whereas continuous variables were expressed as means and standard deviations (minimum–maximum). The Student's t-test was used to compare normally distributed numerical variables between two independent groups, and the Mann–Whitney U test was used for non-normally distributed variables. Receiver operating characteristic (ROC) curves were used to assess the diagnostic performance of the MRI parameters, and the optimal threshold value was identified to maximize sensitivity and specificity in distinguishing malignant from benign lesions. The areas under the ROC (AUROC) curves were calculated, and the difference between two independent AUROC curves was evaluated using z statistics (http://vassarstats.net/roc_comp.html). For all tests, a two-tailed *P* value of less than 0.05 was considered statistically significant.

Results

A total of 70 solid lesions from 50 patients (mean age: 54.3 ± 13.7 years) were included in the evaluation. Of the patients, 16 (32%) were women and 34 (68%) were men. Seventeen patients had multiple lesions (14 had two lesions, and 3 had three lesions) assessed simultaneously. The lesions were classified as benign or malignant based on the histopathology (30%) or typical imaging characteristics and follow-up findings (70%). In total, 20 lesions (28.6%) were classified as benign and 50 lesions (71.4%) as malignant.

Among the benign lesions, 16 (80%) were hemangiomas, 3 (15%) were focal nodular hyperplasia, and 1 (5%) was a hepatocellular adenoma. Among the malignant lesions, 30 (60%) were metastases, 15 (30%) were hepatocellular carcinoma (HCC), 3 (6%) were lymphoma, and 2 (4%) were cholangiocarcinoma. All patients with HCC had chronic liver disease, with 14 diagnosed with cirrhosis.

The mean pre-T1 and post-T1 values were 1,338.8 ± 393.9 and 719.5 ± 260.1 ms, respectively. The mean T2 value was 70.5 ± 19.8 ms. The mean CER was 2.02 ± 0.7, the mean T1D was 634.45 ± 367.44 ms, and the mean percentage T1D was 44.77% ± 17.30%. The mean ADC value was 1.23 ± 0.46 × 10^{-3} mm^2/s, and the mean lesion stiffness was 4.6 ± 1.6 kPa. Malignant lesions had significantly lower T2 , CER, T1D, T1D (%), and ADC values and significantly higher stiffness values ($P < 0.05$). The characteristics of the patient population are summarized in Table 1 and Figure 2.

ROC analysis for the differentiation of malignant versus benign lesions demonstrated that the mean T2, CER, T1D, T1D (%), ADC, and lesion stiffness values all had an AUROC curve greater than 0.6 (Table 2, Figure 3). The mean ADC and lesion stiffness performed slightly better [area under the curve (AUC): 0.861 and 0.848, respectively] than CER, T1D, and T1D (%) (AUC: 0.828, 0.817, and 0.831, respectively) in differentiating malignant from benign lesions. There was no statistically significant difference between the ADC and MRE AUCs for differentiating malignant from benign lesions (z = 0.12, $P = 0.904$).

Discussion

In this study, we evaluated the characteristics of FLLs using mpMRI, DWI, and MRE. We highlighted the effectiveness of these

Table 1. Magnetic resonance imaging characteristics of liver lesions

Parameter	All lesions (n = 70)	Benign lesions (n = 20)	Malignant lesions (n = 50)	*P* value
Pre-T1 value (ms) (n = 70)	1,338.8 ± 393.9 (674–2484)	1,474.9 ± 465.4	1,284.3 ± 351.9	0.110
Post-T1 value (ms) (n = 55)	719.5 ± 260.1 (284–1611)	629.6 ± 230.9	750.2 ± 265.0	0.135
T2 value (ms) (n = 64)	70.5 ± 19.8 (42–122)	82.5 ± 23.3	65.0 ± 15.4	**0.005**
CER (n = 55)	2.02 ± 0.7 (1.04–4.32)	2.71 ± 0.86	1.79 ± 0.52	**0.002**
T1D (ms) (n = 55)	634.5 ± 367.4 (52–1586)	964.0 ± 379.6	521.9 ± 290.6	**<0.001**
T1D (%) (n = 55)	44.8 ± 17.3 (3.96–77.12)	59.4 ± 13.3	39.8 ± 15.7	**<0.001**
ADC (×10^{-3} mm^2/s) (n = 67)	1.23 ± 0.46 (0.290–2.271)	1.60 ± 0.29	1.10 ± 0.43	**<0.001**
MR elastography (kPa) (n = 25)	4.6 ± 1.6 (2.3–8.9)	3.6 ± 1.2	5.4 ± 1.6	**0.004**

Values are presented as mean ± standard deviation, with ranges in parentheses. CER, contrast-enhancement ratio; T1D, T1 relaxation time reduction; T1D (%), T1 relaxation time reduction percentage; ADC, apparent diffusion coefficient.

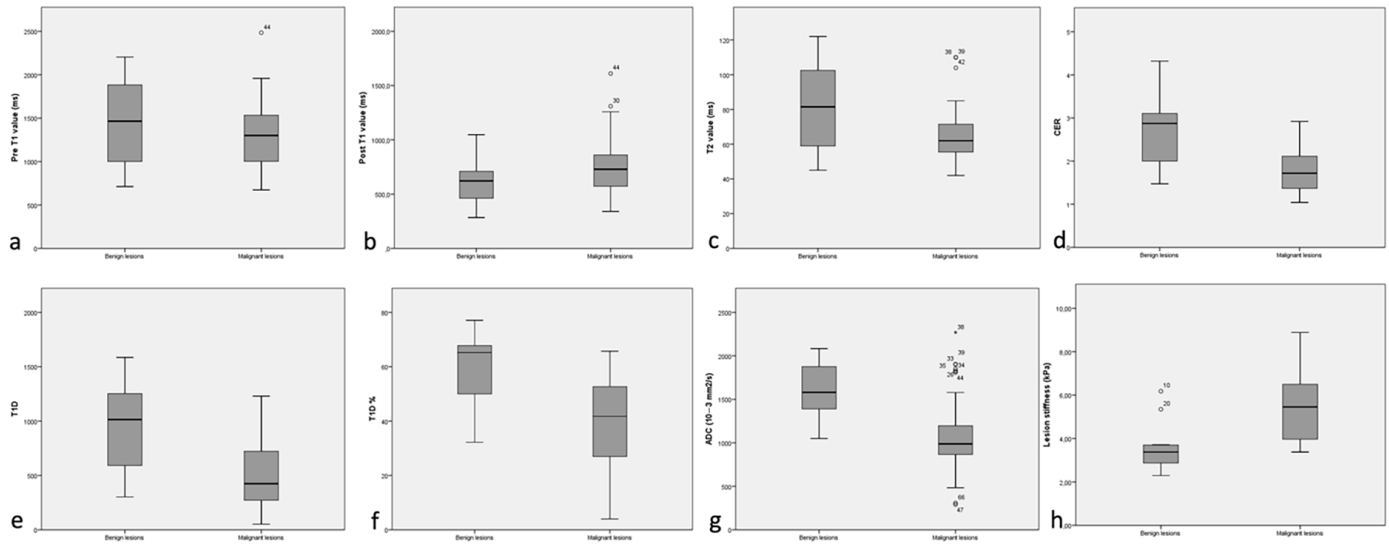

Figure 2. Bar graphs comparing mpMRI, ADC, and MRE measurements between benign and malignant lesions: **(a)** pre-T1 value, **(b)** post-T1 value, **(c)** T2 value, **(d)** CER, **(e)** T1D, (f) T1D (%), **(g)** ADC, **(h)** MRE. mpMRI, multiparametric magnetic resonance imaging, ADC, apparent diffusion coefficient; MRE, magnetic resonance elastography; CER, contrast-enhancement ratio; T1D, T1 relaxation time reduction; T1D (%), T1 relaxation time reduction percentage; ADC, apparent diffusion coefficient.

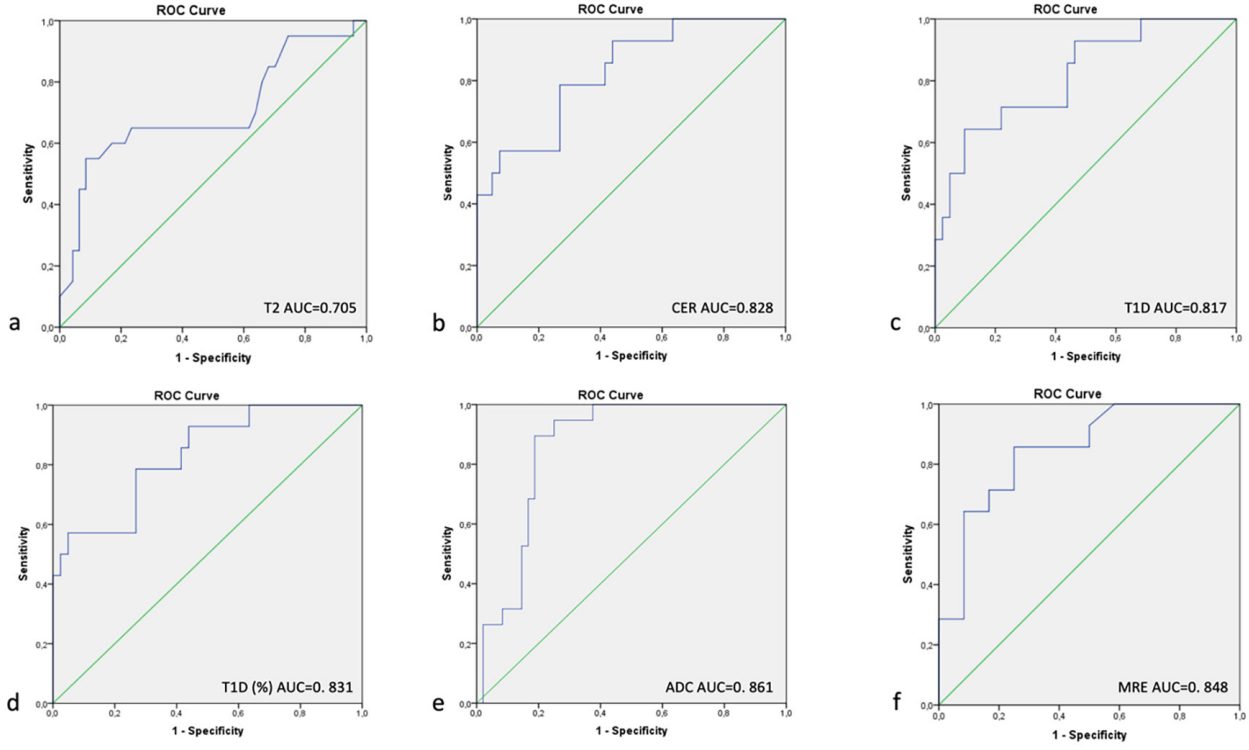

Figure 3. ROC curves for the differentiation of malignant versus benign focal liver lesions: **(a)** T2 relaxation time, **(b)** CER, **(c)** T1D, **(d)** T1D (%), **(e)** ADC, **(f)** MRE. ROC, receiver operating characteristic; CER, contrast-enhancement ratio; T1D, T1 relaxation time reduction; T1D (%), T1 relaxation time reduction percentage; ADC, apparent diffusion coefficient; MRE, magnetic resonance elastography.

imaging techniques in distinguishing between malignant and benign liver lesions. Our findings indicated that malignant lesions had significantly lower T2, CER, T1D, T1D (%), and ADC values while exhibiting significantly higher stiffness values ($P < 0.05$). Notably, the mean ADC and lesion stiffness performed slightly better, with AUC values of 0.861 and 0.848, respectively, compared with T2, CER, T1D, and T1D (%), which had AUC values of 0.705, 0.828, 0.817, and 0.831, respectively, in differentiating malignant from benign liver lesions.

Several studies have investigated the role of mpMRI in differentiating various FLLs. In a previous study, Mio et al.[12] demonstrated that T1 mapping using the phase-sensitive inversion recovery technique was useful for the differential diagnosis of hemangiomas, liver parenchymal cysts, HCC, and metastases. They found that T1D (%) values were high in hemangiomas, similar to our findings, whereas lower values were observed in HCC and metastases. A threshold value >50 was

Table 2. Cut-off values for the differentiation of malignant versus benign liver lesions

Parameter	Cut-off value	AUC (95% CI)	Sensitivity	Specificity
T2 relaxation time (ms)	≤74	0.705 (0.553–0.857)	0.650	0.766
CER	≤1.99	0.828 (0.705–0.950)	0.786	0.732
T1D (ms)	≤749	0.817 (0.687–0.947)	0.714	0.780
T1D (%)	≤49.71	0.831 (0.708–0.954)	0.786	0.732
ADC ($\times 10^{-3}$ mm²/s)	≤1.275	0.861 (0.774–0.948)	0.895	0.812
MR elastography (kPa)	≥3.77	0.848 (0.697–0.999)	0.857	0.750

CER, contrast-enhancement ratio; T1D, T1 relaxation time reduction; T1D (%), T1 relaxation time reduction percentage; ADC, apparent diffusion coefficient; CI, confidence interval; MR, magnetic resonance.

established for differentiating hemangiomas from HCC, achieving 78.8% sensitivity and 100% specificity. A threshold >39 was found to distinguish hemangiomas from metastases, with 60% sensitivity and 97% specificity.

Yoshimura et al.[10] evaluated the role of CER in differentiating metastases from hemangiomas, reporting a threshold value of 1.6, with 100% sensitivity and 95% specificity. Peng et al.[11] assessed the role of T1D and T1D (%) using a dual flip angle VIBE 3D gradient echo sequence for differentiating HCC, focal nodular hyperplasia, and hemangiomas, finding that T1D and T1D (%) were significantly lower in HCC than in hemangiomas, consistent with our study. Wang et al.[13] compared the diagnostic value of T1 mapping and DWI for distinguishing benign and malignant FLLs. Significant differences were observed in native T1, enhanced T1, the percentage change in T1 relaxation time (ΔT1%), and ADC between benign and malignant FLLs. They also reported a similar ADC cut-off value (1.25×10^{-3} mm²/s) for differentiating malignant lesions. Furthermore, they demonstrated that ADC was significantly positively correlated with T1 and ΔT1% and negatively correlated with enhanced T1.

Only one study has directly compared T2 values between malignant and benign FLLs, reporting significantly lower T2 and ADC values in malignant lesions. The researchers found a higher AUC for T2 (0.932), with a cut-off value of 107 ms, compared with an AUC of 0.874 for ADC with a cut-off of 1.25×10^{-3} mm²/s.[14] In our study, however, the AUC for ADC was higher than in that report.

In our study, the threshold stiffness value for differentiating benign and malignant lesions was found to be 3.77 kPa or higher, with a sensitivity of 85% and specificity of 75%. Previous studies have reported similar findings regarding the differentiation of malignant and benign FLLs using MRE. Venkatesh et al.[7] conducted a preliminary study, revealing that malignant lesions had higher stiffness values, with a threshold of 5 kPa and 100% accuracy. Dominguez et al.[15] reported that benign and malignant liver lesions could be distinguished using a threshold value of 5.78–5.82 kPa, achieving 75%–85% accuracy, 64.7%–82.8% sensitivity, and 88% specificity. Another study by Hennedige et al.[8] evaluated 124 FLLs with MRE and DWI and observed significantly higher accuracy for MRE than for DWI (0.986 vs. 0.82, $P = 0.0016$). Abdelgawad et al.[16] also evaluated 124 FLLs using MRE and DWI. They found a strong negative correlation between the ADC of FLLs and MRE stiffness and reported a cut-off value of 4.23 kPa, with an AUC of 0.991 for MRE and a cut-off value of 1.43×10^{-3} mm²/s with an AUC of 0.894 for DWI. Our study, based on a limited number of patients, observed similar AUCs for ADC and MRE, with no statistically significant difference.

The current study has several strengths and limitations. This is the first study to evaluate mpMRI, DWI, and MRE for differentiating malignant versus benign liver lesions, demonstrating various AUCs and enabling comparisons within the same population. The number of included lesions was limited, with most diagnosed based on follow-up rather than histopathologic evaluation. The retrospective nature of the study also led to restricted availability of MRE data for some lesions. However, the statistically significant findings, consistent with previous studies, underscore the importance of MRE in the differential diagnosis of benign and malignant FLLs. Additionally, subgroup analyses were not performed due to the limited sample size in each group. This highlights the need for more comprehensive prospective studies with a homogeneous distribution of lesion types to further clarify the role of mpMRI, DWI, and MRE in the characterization of FLLs.

In conclusion, mpMRI, DWI, and MRE can be used for the differentiation of solid liver lesions, with ADC and lesion stiffness performing slightly better than CER, T1D, and T1D (%). Comprehensive future studies involving a larger number of patients and lesions will enable the comparison of different techniques and demonstrate the impact of their combined application on diagnostic accuracy.

Footnotes

Conflict of interest disclosure

The authors declared no conflicts of interest.

References

1. Pang EH, Harris AC, Chang SD. Approach to the solitary liver lesion: imaging and when to biopsy. *Can Assoc Radiol J*. 2016;67(2):130-148. [Crossref]
2. Hodler J, Kubik-Huch RA, von Schulthess GK, editors. Diseases of the Abdomen and Pelvis 2018-2021: Diagnostic Imaging - IDKD Book [Internet]. Cham (CH): Springer; 2018. [Crossref]
3. Taouli B, Koh DM. Diffusion-weighted MR imaging of the liver. *Radiology*. 2010;254(1):47-66. [Crossref]
4. Idilman IS, Li J, Yin M, Venkatesh SK. MR elastography of liver: current status and future perspectives. *Abdom Radiol (NY)*. 2020;45(11):3444-3462. [Crossref]
5. Banerjee R, Pavlides M, Tunnicliffe EM, et al. Multiparametric magnetic resonance for the non-invasive diagnosis of liver disease. *J Hepatol*. 2014;60(1):69-77. [Crossref]
6. Thomaides-Brears HB, Lepe R, Banerjee R, Duncker C. Multiparametric MR mapping in clinical decision-making for diffuse liver disease. *Abdom Radiol (NY)*. 2020;45(11):3507-3522. [Crossref]
7. Venkatesh SK, Yin M, Glockner JF, Takahashi N, Araoz PA, Talwalkar JA, Ehman RL. MR elastography of liver tumors: preliminary results. *AJR Am J Roentgenol*. 2008;190(6):1534-1540. [Crossref]
8. Hennedige TP, Hallinan JT, Leung FP, et al. Comparison of magnetic resonance elastography and diffusion-weighted imaging for differentiating benign and malignant liver lesions. *Eur Radiol*. 2016;26(2):398-406. [Crossref]
9. Hectors SJ, Wagner M, Bane O, et al. Quantification of hepatocellular carcinoma heterogeneity with multiparametric magnetic resonance imaging. *Sci Rep*. 2017;7(1):2452. [Crossref]

10. Yoshimura N, Saito K, Saguchi T, et al. Distinguishing hepatic hemangiomas from metastatic tumors using T1 mapping on gadoxetic-acid-enhanced MRI. *Magn Reson Imaging*. 2013 Jan;31(1):23-27. [Crossref]

11. Peng Z, Li C, Chan T, et al. Quantitative evaluation of Gd-EOB-DTPA uptake in focal liver lesions by using T1 mapping: differences between hepatocellular carcinoma, hepatic focal nodular hyperplasia and cavernous hemangioma. *Oncotarget*. 2017;8(39):65435-65444. [Crossref]

12. Mio M, Fujiwara Y, Tani K, Toyofuku T, Maeda T, Inoue T. Quantitative evaluation of focal liver lesions with T1 mapping using a phase-sensitive inversion recovery sequence on gadoxetic acid-enhanced *MRI. Eur J Radiol Open*. 2020;8:100312. [Crossref]

13. Wang F, Yang Q, Zhang Y, Liu J, Liu M, Zhu J. 3D variable flip angle T1 mapping for differentiating benign and malignant liver lesions at 3T: comparison with diffusion weighted imaging. *BMC Med Imaging*. 2022;22(1):146. [Crossref]

14. Cieszanowski A, Anysz-Grodzicka A, Szeszkowski W, et al. Characterization of focal liver lesions using quantitative techniques: comparison of apparent diffusion coefficient values and T2 relaxation times. *Eur Radiol*. 2012;22(11):2514-24. [Crossref]

15. Dominguez A, Fino D, Spina JC, et al. Assessment of SE-MRE-derived shear stiffness at 3.0 Tesla for solid liver tumors characterization. *Abdom Radiol (NY)*. 2021;46(5):1904-1911. [Crossref]

16. Abdelgawad MS, Elseady BA, ELabd OL, Kohla MS, Samea MESA. Comparison of magnetic resonance elastography and diffusion-weighted imaging for differentiating benign and malignant liver lesions. *Egypt J Radiol Nucl Med*. 2024;55. [Crossref]